The Light Transmittance and Electrical Conductivity Properties of Gelam Wood Carbon Nanosheet and Its Derivatives

by Dedi Rohendi

Submission date: 07-Oct-2022 02:52PM (UTC+0700)
Submission ID: 1919035278
File name: roperties_of_Gelam_Wood_Carbon_Nanosheet_and_Its_Derivatives.pdf (366.3K)
Word count: 3473
Character count: 18695

IJFAC

Indonesian Journal of Fundamental and Applied Chemistry

Article http://ijfac.unsri.ac.id

The Light Transmittance and Electrical Conductivity Properties of Gelam Wood Carbon Nanosheet and Its Derivatives

Nyimas Febrika Syabania[1], Nirwan Syarif[2]*, Dedi Rohendi[2,3], Mellysa Wandasari[3], and Wara Dyahpita Rengga[4]

[1]Magister Program of Chemistry, Faculty of Mathematics and Natural Sciences, Sriwijaya University
[2]Department of Chemistry, Faculty of Mathematics and Natural Sciences, Sriwijaya University
[3]National Center for Sustainable Transportation Technology, Bandung, Indonesia
[4]Department of Chemical Engineering, UniversitasNegeri Semarang, Semarang, Jateng, Indonesia

*Corresponding Author: nsyarif@unsri.ac.id

Article Info
Received 22 April 2019
Received in revised 7 May 2019
Accepted 21 May 2019
Available online 10 October 2019

Abstract

The research on the preparation and characterization of transparent electrode carbon nanosheet based gelam woods bark doped with SnO_2-SbO_2. XRD analysis showed peaks at 2θ = 26.87°; 26.38° for carbon crystal and at 2θ = 33.59°; 34.35° for SnO; at 2θ = 51.99°; 62.20° for SbO_2. SEM analysis show that the carbons have self-curling sheets that indicated defection in their surface. The carbons have self-curling sheets, which indicated that their surfaces have many defect. It assumed when exfoliation process undergone, the layers was significantly decreased as sonication process and formed rCNSO. Diffractogram XRD of CNS, CNSO and rCNSO showed diffraction peak at 2θ= 24.3°. Oxygen functional group in CNSO might cause an increasing of interlayers distance between hexagonal networks of carbon layer. It also affect electrical resistant or the conductivity. FTIR spectrum indicate that CNSO has several absorption peaks at for –OH stretch for free water and alcohol. At 2337 cm^{-1} was showed a carboxylic acid peak and C=C stretch at 1627 cm^{-1}. There is a skeletal vibration rCNSO structure occurred at each graphene layers. The ratio of the integrated intensities (I_G/I_D = 0.89 for CNS, 0.85 for CNS-O, and 0.93 for rCNSO of Raman spectroscopy is significantly high. Electrical conductivity of transparent electrode ranges from 1.26 x 10^{-7} Scm^{-1} – 5.03 x $10^{-7}$$Scm^{-1}$. The highest conductivity value on transparent electrode contained rCNSO. This result inferred that the usage of rCNSO can increase electrical conductivity. Therefore, the higher value of electrical conductivity can be related to the value of L_a. The average maximum absorption wavelength is observed at 350-510 nm which means that the transition of the electronic transition π→π* occurs in the conjugated carbons system. Electrical conductivity of transparent electrode ranges from 1.26 x 10^{-7} Scm^{-1} – 5.03 x 10^{-7} Scm^{-1}. The highest conductivity value on transparent electrode contained rCNSO. The band gap values in the transparent electrode range from 2 eV - 3 eV which means they have conductor – semiconductor characters.

Keywords: Nanosheet, Carbon, Electrical, Conductivity, Derivate.

INTRODUCTION

Transparent electrode is a device that has the ability to deliver electricity and light simultaneously. Generally, transparent electrodes are made of glass coated with indium-tin oxide. The use of indium-tin oxide has a technical deficiency of very limited survival of about 14,000 hours, Indium tin oxide is easily damaged if exposed to water. The development of improved sealing process in the practice of making transparent electrodes can limit the durability of the display, but the intensity of the transmitted light (transparency) has not been high enough. Indium as part of transparent electrode, found as earth rare metal. These facts promoted alternative search for transparent electrode materials. One of such alternative is carbon nanosheet [1].

Carbon nanosheet exhibited various electronic properties and magnetic properties that has significant implications for applications in the semiconductor industry [2]. Previously, we prepared carbon nanosheet from gelam wood bark [3]. The carbon material was conductive and showed good electrochemical performance. Preliminary study showed that composite of epoxy resin and gelam wood carbon nanosheet has capacitive property. Capacitance is one factor that contributing transparent electrode performance, besides conductivity and transparency. Therefore, the application of gelam wood carbon nanosheet in

transparent electrode is reliable. This paper reports the preparation of gelam wood carbon nanoribbon and its derivatives; and its transmittance and electrical conductivity.

MATERIALS AND METHODS

Materials

The materials used in this study were Gelam wood bark,SnO_2, K_2SbO_2, FT-IR (Shimadzu 2450), X-Ray Diffraction (XRD) diffractograms (Rigaku Miniflex 600, SEM (JSM 6510A).

Methods

Carbon Preparation

The starting materials to prepare carbon nanosheet powder were gelam wood bark which is a waste from the carpentry and wood industry. Gelam wood bark was separated from the wood and cleaned with flowing clean water and was removed from organic impurities with hot water. Gelam wood bark was milled into powder using disk mill from JIMO FF-15 and processed into carbon using hydrothermal assisted microwave pyrolysis. The procedure can be found elsewhere[4]. The process produced carbon nanosheet (CNS). CNS was oxidized to form carbon nanosheet oxide (CNSO) by using Hummer methods. Detail explanation about Hummer method can be found in related paper [5]. CNSO was exfoliate to reduced layer and size through sonication for 30 minutes and then heated in the electric oven 120 ˚C for 2 hours to form reduced CNSO (rCNSO). CNS, CNSO and rCNSO were proceed to characterize their light transmittance and electrical conductivity.

Light Transmittance and Electrical Conductivity Characterizations

Glass of 3 mm thick was cut with size 4 x 1 cm and then washed for 10 minutes in beaker containing methanol. The washed glass was placed on top of a piece ceramic to be heated in the furnace for 10 minutes with temperature of 600 °C. A 100 mL solution of SnCl2 and K2SbO2 mixture (1:1) in DMSO was put into the spray tube and was sprayed to the glass and the glass was put back into the furnace for 2 minutes to reheat. The heating formed $SnO_2 - SbO_v$ in the surface of glass and acted as dopant for carbon (CNS, CNSO and rCNSO) to produced transparent electrodes. Transparent electrodes were subjected into FTIR, XRD, SEM, UV–Vis and impedance spectroscopy instrumentations for functionality, crystallography, morphology, light transmittance and electrical conductivity, respectively. FTIR spectra was obtained from Shimadzu 2450. X-Ray Diffraction (XRD) diffractograms were plotted by using Rigaku Miniflex 600 with CuKα radiation. SEM images were produced from type JSM 6510 A. Light transmittance was determined from UV– Vis spectra with wavelength range 300 - 800 nm.

Band gap energy was calculated using maximum and minimum light transmittance and converted into index bias value using formula (1), thin layer bias value (2), thickness of thin layer (3) and light transmittance coefficient (4) [6].

$$N = 2n_s \frac{T_M - T_m}{T_M T_m} + \frac{n_s^2 + 1}{2} \quad \text{.....(1)}$$

$$n = n_s^2 + \sqrt{N + \sqrt{N^2}} \quad \text{.....(2)}$$

$$d = \frac{\lambda_1 \lambda_2}{2(\lambda_1 n_2 - \lambda_2 n_1)} \quad \text{.....(3)}$$

$$\alpha = \frac{1}{d} lnT \quad \text{.....(4)}$$

where hυ = hc/λ, h = 6.63 x 10 -34 Js, c = 3 x 108 ms and λ = 300 to 700 10-9 m. Direct energy gap (λhυ)2 is derived from graph extrapolation between the energy α versus hυ at α = 0.

RESULT AND DISCUSSION

Thermal decomposition occurs in limited amount or absence of oxygen in the pyrolysis process, make all organic matters turn into carbon. Microwave pyrolysis uses the energy adsorbent in the mixture, so that makes temperature increasing drastically. Figure 1A shows the yield (CNS) of microwave pyrolysis in 800 °C and for 25 minutes. Oxidizing CNS produced CNSO (Carbon nanosheet oxide), and reducing of CNS-O obtained rCNSO. Visual characteristic was an initial indicator to determine CNS, CNSO or rCNSO. It can be shown from Fig. 1 that the colour of solution change from green to light brown and to black. A black, hygroscopic, brittle and soft precipitate of rCNSO has been obtained after thermal heating process in 120 °C.

Carbon Preparation

Figure 1 show SEM images of CNS, CNSO and rCNSO. It can be shown that the carbons have self-curling sheets which indicated that their surfaces have many defect. It assumed when exfoliation process undergone, the layers was significantly decreased as sonication process and formed rCNSO.

XRD spectra of CNS, CNSO and rCNSO (Figure 2) showed diffraction peak at 2θ = 24.3° . This fact confirmed that the rCNSO formation has been prepared as the same with Liu et al (2012) from reduction of CNSO by using ethylene glycol. A broaden peak was indicated asymmetry layers in rCNSO lattice after exfoliation process. Therefore, a defect in crystalline of carbon was formed. A broad and strong intensity peak was shown in rCNSO at 2θ = 25.9°.

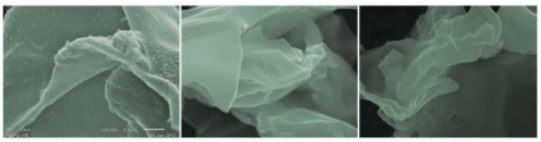

(a) (b) (c)

Figure 1. SEM images of (a) CNS, (b) CNSO and (c) rCNSO

rCNSO was formed as similar to Blanton and Majumdar in JCPDS-ICDD [7] with graphite flake as precursor that has peaks laid between 23-24°. CNSO was occurred as thermal heating at 120 °C. It can be shown that the oxidation of oxide functiona groups give peak at 10degree of diffractogram both for CNSO and graphite oxide.

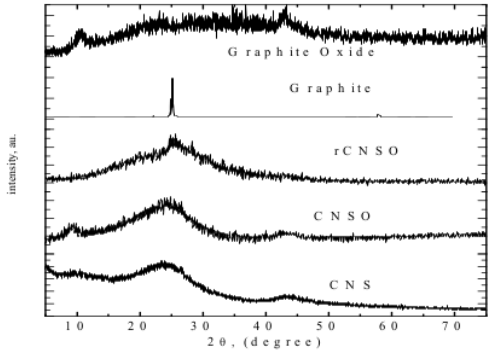

Figure 2. XRD Diffractograms for CNS, CNSO, rCNSO, graphite and graphite oxide

Oxygen functional group in CNSO might cause an increasing of interlayers distance between hexagonal networks of carbon layer. It also affect electrical resistant or the conductivity. Therefore, the reduction process was able to minimize the gap [8]. Value of d-spacing (Table 1) was calculate by Brag's law and particle sized by Debye Scheerer method. Full Width Half Maximum (FWHM) of each peaks was inversely proportional to its particle size due to the ordering of crystalline. A small particle size might has a low particle ability in destructing the barrier of incident light therefore, a broad peaks was occurred.

Table 1. Particle Size Number And D-Spacing

Carbon type	FWHM	θ	nm	d-spacing
Graphite	8.83	1.94	0.92	0.38
Grapheneoxide	11.03	25.90	0.74	0.35
CNS	0.46	23,60	17.77	0.34
CNSO	0.23	28.30	35.01	0.32
rCNSO	1.94	7.70	4.10	1.15

FTIR spectrograms indicate that CNSO has several absorption peaks at for –OH stretch for free water and alcohol. At 2337 cm^{-1} was showed a carboxylic acid peaks and C=C stretch at 1627 cm^{-1}. Hence, it confirmed that there is a skeletal vibration rCNSO structure occurred at each graphene layers. At fingerprint area of epoxy and alkoxy groups show up at 1172 and 1056 cm^{-1}.

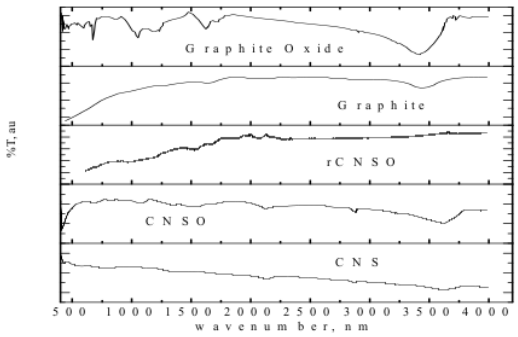

Figure 3. FTIR Spectrogram for CNS, CNSO, rCNSO, graphite and graphite oxide

Raman spectroscopy analysis (Figure 4) was employed to further investigate the structure of the CNS, CNSO and rCNSO. It can be shown that all samples exhibit abroad disorder-induced D_{band} (~1330 cm^{-1}) and in-plane vibrational G_{band} (~1590 cm^{-1}). In all of the CNS, the intensity of the G_{band} is significantly higher than that of the D_{band}, indicating that the CNS are partially graphitized.

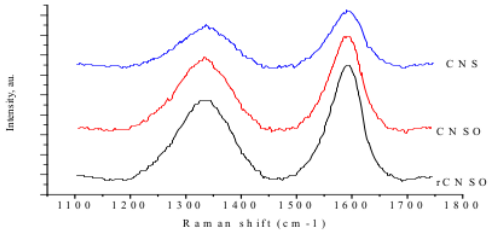

Figure 4. Raman Spectrogram for CNS, CNSO and rCNSO.

The ratio of the integrated intensities (IG/ID = 0.82 for CNS, 0.85 for CNSO, and 0.93 for rCNSO is significantly higher than for the commercial activated carbon (Norit, IG/ID = 0.52 (AC)). It is known that the K of $KMnO_4$ acts to attack the aligned (i.e., graphitic) structural domains in a carbon matrix, resulting in a highly intercalation but disordered structure (figure 4(b)) with relatively poor electrical conductivity. The K-intercalation CNS samples show a relatively high

degree of graphitization, which is related to the intrinsic complex hierarchical structure of the precursor. As discussed earlier, gelam wood bark fiber contains a high content of crystalline cellulose. During the high temperature, pyrolysis leads to structural alignment, while the breakdown of aligned structural domains occurs due to the K-intercalation.

The degree of graphitic content in the carbons were resulted from these simultaneous processes. The highest relative of IG/ID ratio can be found in rCNSO and the lowest is in CNS. This found can suggest that there is a competition between oxidation reduction induced ordering and diverse functionality induced disorder in carbon structure [9]. Table 1 shows the calculated mean width (L_a) of the graphitic domains in each specimen, which is proportional to the IG/ID ratio. The higher value of L_a indicates higher electrical conductivity can be expected.

Light Transmittance and Electrical Conductivity

The effect of coated glass with CNS, CNSO and rCNSO in light transmittance and electrical conductivity of the glass to form transparent electrodes, can be seen in Table 1. The electrical conductivity values were derived from the current value and resistance obtained from the measurement of the transparent electrode connected to the electrochemical impedance instrumentation.

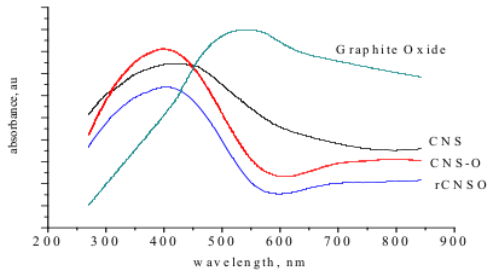

Figure 5. UV-Vis Spectrogram for CNS, CNSO, rCNSO and Graphite Oxide

Electronic properties of material can be represented as band gap value. The value can be calculated using Tauc formula. Tauc formula starts from the characterization of optical properties by determining the maximum and minimum transmittance value at certain wavelengths. The result of transmittance with UV-Vis spectrometer is shown in figure 6. The figure shows a sharply transmittance change in the 300-800 nm wavelength range which is the area of visible light to ultraviolet wavelength. The change in intensity indicates a high absorption / transmittance at that wavelength.

Based on the graphs generated from the four images shows the maximum wavelength difference on each composition of the transparent electrode. This is due to the influence of spray plate thickness on each of the different transparent electrode. It is also influenced by the presence of hexagonal structures in the CNS increase tight filler electrode surface, making the rays passing through the transparent electrode will increasingly vary on each composition so as to produce different maximum wavelengths. The average maximum absorption peak on a transparent electrode is from the wavelength range 350-600 nm. The average maximum absorption wavelength is observed at 350-530 nm which means that the transition of the electronic transition $\pi \rightarrow \pi^*$ occurs in the conjugated carbon system of CNS, in addition there is also a maximum absorption peak at 600-620 nm range i.e., transition electronic $n \rightarrow \pi^*$ is indicated by the presence of electrons pair that come from polyaniline. The wavelength absorption shift occurs in CNSO and rCNSO (Figure 5 (b) and (c), respectively) due to thickness change in CNS (Figure 5(a)), which if the smaller metal size resulted in its absorption toward the greater wavelength.

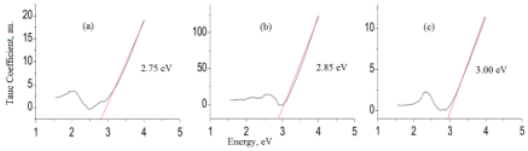

Figure 6. Bandgap extrapolation (red lines) from Tauc plot (black lines) of transparent electrode CNS, CNSO, and rCNSO.

Figure 6 shows that the band gap values in the transparent electrode range from 2 eV - 3 eV which means they have conductor – semiconductor characters. This found confirmed the result from Choudhury [10] that CNS can change from conductor to semiconductor or vice versa. The lowest band gap value, i.e. 2.75 eV came from transparent electrode that content CNS. It can be understand because CNS has lowest conductivity that related to other band gap.

CONCLUSION

Carbon nanosheet can be obtained from microwave pyrolysis in 800 °C, for 25 minutes. Oxidizing CNS produced CNSO (Carbon nanosheet oxide), and reducing of CNSO obtained rCNSO. Visual characteristic was an initial indicator to determine CNS, CNSO or rCNSO. The colour of solution change from green to light brown and to black. A black, hygroscopic, brittle and soft precipitate of rCNSO has been obtained after thermal heating

process in 120 °C. The carbons have self-curling sheets, which indicated that their surfaces have many defect. It assumed when exfoliation process undergone, the layers was significantly decreased as sonication process and formed rCNSO. XRD spectra of CNS, CNSO and rCNSO showed diffraction peak at 2θ= 24.3°. Oxygen functional group in CNSO might cause an increasing of interlayers distance between hexagonal networks of carbon layer. It also affect electrical resistant or the conductivity. FTIR spectrograms indicate that CNSO has several absorption peaks at for –OH stretch for free water and alcohol. At 2337 cm^{-1} was showed a carboxylic acid peaks and C=C stretch at 1627 cm^{-1}. There is a skeletal vibration rCNSO structure occurred at each graphene layers. The ratio of the integrated intensities (IG/ID = 0.89 for CNS, 0.85 for CNS-O, and 0.93 for rCNSO of Raman spectroscopy is significantly high. Electrical conductivity of transparent electrode ranges from 1.26 x 10-7 Scm^{-1} – 5.03 x 10-7 Scm $^{-1}$. The highest conductivity value on transparent electrode contained rCNSO. This result inferred that the usage of rCNSO can increase electrical conductivity. Therefore, the higher value of electrical conductivity can be related to the value of La. The average maximum absorption wavelength is observed at 350-530 nm which means that the transition of the electronic transition $\pi \rightarrow \pi^*$ occurs in the conjugated carbons system. Electrical conductivity of transparent electrode ranges from 1.26 x 10-7 Scm-1 – 5.03 x 10-7 Scm^{-1}. The highest conductivity value on transparent electrode contained rCNSO. The band gap values in the transparent electrode range from 2 eV - 3 eV which means they have conductor – semiconductor characters.

ACKNOWLEDGMENT

All acknowledgments (if any) should be included at the very end of the paper before the references and may include supporting grants, presentations, and so forth.

REFERENCES

[1] Goessens A, Satyanarayana B, Van der Stocken T, Quispe Zuniga M, Mohd-Lokman H, Sulong I and Dahdouh-Guebas F. "Is Matang Mangrove Forest in Malaysia sustainably rejuvenating after more than a century of conservation and harvesting management?," *PLoS ONE.*, vol. 9, no. 8, 2014.

[2] Spence, Kelley L., Richard A. Venditti, Youssef Habibi, Orlando J. Rojas, and Joel J. Pawlak. "The effect of chemical composition on microfibrillar cellulose films from wood pulps: mechanical processing and physical properties." *Bioresource technology*, vol. 101, no. 15 pp. 5961-5968, 2010.

[3] Salajkova, Michaela, Luca Valentini, Qi Zhou, and Lars A. Berglund. "Tough nanopaper structures based on cellulose nanofibers and carbon nanotubes." *Composites Science and Technology.*, vol. 87, pp. 103-110, 2013.

[4] Xu, Chengyong, Paul A. Brown, and Kevin L. Shuford. "Strain-induced semimetal-to-semiconductor transition and indirect-to-direct band gap transition in monolayer 1T-TiS 2." *RSC Advances.*, vol.5, no. 102, pp. 83876-83879, 2015.

[5] Boehm, H. P. "Some aspects of the surface chemistry of carbon blacks and other carbons." *Carbon*, vol. 32, no. 5, pp. 759-769, 1994.

[6] Lim, Way F., and Kuan Y. Cheong. "Effects of post-deposition annealing temperature on band alignment and electrical characteristics of lanthanum cerium oxide on 4H-SiC." *MRS Online Proceedings Library Archive*, vol. 1433, 2012.

[7] Segets, Doris, J. Matthew Lucas, Robin N. Klupp Taylor, Marcus Scheele, Haimei Zheng, A. Paul Alivisatos, and Wolfgang Peukert. "Determination of the quantum dot band gap dependence on particle size from optical absorbance and transmission electron microscopy measurements." *ACS Nano.*, vol. 6, no. 10, pp. 9021-9032, 2012.

[8] Baraton, M. "Optimizing chemical gas sensors using ir spectroscopy." *SPIE Newsroom*, 2009.

[9] Huang, Ting, Bo Jin, Ru Peng, Cong Chen, Rong Zheng, Yi He, and Shi Chu. "Synthesis and characterization of [60] fullerene-glycidyl azide polymer and its thermal decomposition." *Polymers*, vol. 7, no. 5, pp. 896-908, 2015.

[10] Kim, Ki Kang, Soo Min Kim, and Young Hee Lee. "Chemically conjugated carbon nanotubes and graphene for carrier modulation." *Accounts of chemical research* 49, no. 3 (2016): 390-399.

[11] Liu, Changqing, and Guoxin Hu. "Effect of nitric acid treatment on the preparation of graphene sheets by supercritical N, N-dimethylformamide exfoliation." *Industrial & Engineering Chemistry Research,* vol. 53, no. 37, pp. 14310-14314, 2014.

[12] Jeong, H. K., M. H. Jin, K. P. So, S. C. Lim, and Y. H. Lee. "Tailoring the characteristics of graphite oxides by different oxidation times." *Journal of Physics D: Applied Physics*, vol. 42, no. 6, pp. 065418, 2009.

[13] Qin, Wei, Jiechang Hou, and Dawn A. Bonnell. "Effect of interface atomic structure on the electronic properties of nano-sized metal–oxide

interfaces." *Nano letters*., vol. 15, no. 1, pp. 211-217, 2014.

[14] Van Diepen, A. M., and Th JA Popma. "Temperature dependence of the hyperfine field in amorphous Fe2O3." *Solid State Communications*., vol. 27, no. 2 , pp. 121-125, 1978.

[15] Su, Dawei, Mike Ford, and Guoxiu Wang. "Mesoporous NiO crystals with dominantly exposed {110} reactive facets for ultrafast lithium storage." *Scientific reports*., vol. 2, pp. 924, 2012.

[16] Anh Huy, Huynh, Bálint Aradi, Thomas Frauenheim, and Peter Deák. "Comparison of Nb- and Ta-doping of anatase TiO2 for transparent conductor applications." .,2012.

The Light Transmittance and Electrical Conductivity Properties of Gelam Wood Carbon Nanosheet and Its Derivatives

ORIGINALITY REPORT

21%	19%	11%	4%
SIMILARITY INDEX	INTERNET SOURCES	PUBLICATIONS	STUDENT PAPERS

PRIMARY SOURCES

1	eprints.unsri.ac.id Internet Source	10%
2	www.freepatentsonline.com Internet Source	4%
3	Huanlei Wang, Zhanwei Xu, Alireza Kohandehghan, Zhi Li et al. "Interconnected Carbon Nanosheets Derived from Hemp for Ultrafast Supercapacitors with High Energy", ACS Nano, 2013 Publication	2%
4	Submitted to Fakultas Ekonomi dan Bisnis Universitas Gadjah Mada Student Paper	2%
5	sativa-power.de Internet Source	1%
6	cmsdata.iucn.org Internet Source	1%
7	www.scilit.net Internet Source	1%

8	insightsociety.org Internet Source	1%

Exclude quotes	On	Exclude matches	< 1%
Exclude bibliography	On		